Journal of Inorganic Biochemistry 253 (2024) 112484

Contents lists available at ScienceDirect

Journal of Inorganic Biochemistry

journal homepage: www.elsevier.com/locate/jinorgbio

Hole-scavenging in photo-driven N_2 reduction catalyzed by a CdS-nitrogenase MoFe protein biohybrid system

Andrew Clinger [a,1], Zhi-Yong Yang [a,1], Lauren M. Pellows [b], Paul King [c], Florence Mus [d], John W. Peters [d], Gordana Dukovic [b,e,f], Lance C. Seefeldt [a,*]

[a] Department of Chemistry and Biochemistry, Utah State University, Logan, UT 84322, United States of America
[b] Department of Chemistry, University of Colorado Boulder, Boulder, CO 80309, United States of America
[c] Biosciences Center, National Renewable Energy Laboratory, Golden, CO 80401, United States of America
[d] Department of Chemistry and Biochemistry, University of Oklahoma, Norman, OK 73019, United States of America
[e] Materials Science and Engineering, University of Colorado Boulder, Boulder, CO 80303, United States of America
[f] Renewable and Sustainable Energy Institute (RASEI), University of Colorado Boulder, Boulder, CO 80303, United States of America

ARTICLE INFO

Keywords:
Nitrogenase
CdS-MoFe protein biohybrid
electron donor
Light-driven

ABSTRACT

The light-driven reduction of dinitrogen (N_2) to ammonia (NH_3) catalyzed by a cadmium sulfide (CdS) nanocrystal-nitrogenase MoFe protein biohybrid is dependent on a range of different factors, including an appropriate hole-scavenging sacrificial electron donor (SED). Here, the impact of different SEDs on the overall rate of N_2 reduction catalyzed by a CdS quantum dot (QD)-MoFe protein system was determined. The selection of SED was guided by several goals: (*i*) molecules with standard reduction potentials sufficient to reduce the oxidized CdS QD, (*ii*) molecules that do not absorb the excitation wavelength of the CdS QD, and (*iii*) molecules that could be readily reduced by sustainable processes. Earlier studies utilized buffer molecules or ascorbic acid as the SED. The effectiveness of ascorbic acid as SED was compared to dithionite (DT), triethanolamine (TEOA), and hydroquinone (HQ) across a range of concentrations in supporting N_2 reduction to NH_3 in a CdS QD-MoFe protein photocatalytic system. It was found that TEOA supported N_2 reduction rates comparable to those observed for dithionite and ascorbic acid. HQ was found to support significantly higher rates of N_2 reduction compared to the other SEDs at a concentration of 50 mM. A comparison of the rates of N_2 reduction by the biohybrid complex to the standard reduction potential (E^o) of the SEDs reveals that E^o is not the only factor impacting the efficiency of hole-scavenging. These findings reveal the importance of the SED properties for improving the efficiency of hole-scavenging in the light-driven N_2 reduction reaction catalyzed by a CdS QD–MoFe protein hybrid.

1. Introduction

The enzyme nitrogenase catalyzes all biological reduction of dinitrogen (N_2) to ammonia (NH_3), the largest contributor of fixed nitrogen into the biosphere [1,2]. Nitrogenase, found widely across the bacterial and archaeal domains of life, is known to exist in three isoforms [3–5], with the Mo-dependent isoform being the most widely distributed, best studied, and paradigm for the group [3,4,6–10]. The Mo-nitrogenase is composed of two component proteins, called the MoFe protein and Fe protein, that work together to reduce N_2 (Fig. 1). The delivery of each electron from the Fe protein to the MoFe protein is coupled to the hydrolysis of at least 2 ATP molecules to 2 ADP + 2 Pi molecules [11–13]. This requirement for ATP hydrolysis represents a significant energy demand, limiting utilization of nitrogenase for generation of fixed nitrogen [14]. Efforts in recent years have been directed at delivering electrons to the MoFe protein without the need for the Fe protein and ATP hydrolysis [9,15–17]. Earlier studies with a MoFe protein with amino acid substitutions showed reduction of hydrazine to ammonia using Eu(II)-ligand complexes as reductant [16,17]. More recently, studies with wild-type MoFe protein have shown that it is possible to connect the MoFe protein to an electrode as the source of electronsto drive N_2 reduction to NH_3, although as yet the rates of N_2 reduction are very low [18]. It has also been demonstrated that photo-driven electron transfer within a cadmium sulfide (CdS) nanocrystal (NC) as either

* Corresponding author.
E-mail address: lance.seefeldt@usu.edu (L.C. Seefeldt).
[1] Authors contributed equally.

https://doi.org/10.1016/j.jinorgbio.2024.112484
Received 14 November 2023; Received in revised form 5 January 2024; Accepted 8 January 2024
Available online 9 January 2024

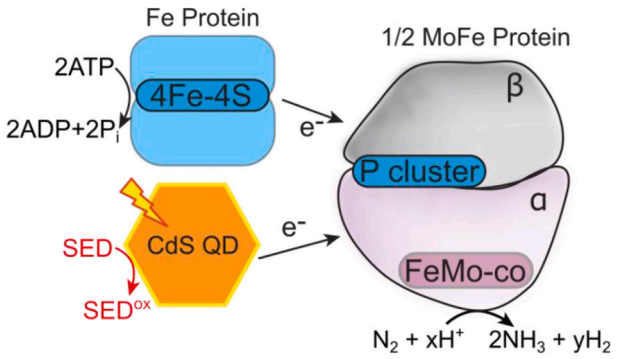

Fig. 1. Cartoon depiction of electron delivery to the MoFe protein of nitrogenase from either the Fe protein component of nitrogenase or from photoexcited CdS quantum dots (CdS QD), with electrons provided by a sacrificial electron donor (SED). CdS QD can reduce both the P cluster and FeMo-co, with transfer from the P cluster to FeMo-co unknown in this system.

nanorod (NR)- or quantum dot (QD)–MoFe protein biohybrid complexes can achieve significant rates of N_2 reduction, thereby allowing the use of renewable solar energy to drive the reaction and eliminating the need for ATP hydrolysis [19,20]. In these complexes, absorption of light by the CdS nanocrystal excites an electron from the valence band to the conduction band, creating a strong reductant that can transfer an electron to a bound MoFe protein (Fig. 1) [21]. The transfer of an electron results in an oxidized CdS QD, leaving behind a positively charged hole in the valence band that must be scavenged by an electron-donating small molecule (sacrificial electron donor (SED)), to regenerate the resting state CdS QD [22–24]. Among the many factors that are essential to the achieving N_2 reduction in a photo-driven biohybrid, the rate of hole-scavenging by SED is an important one. The earlier work demonstrating that a productive complex between CdS QD and nitrogenase MoFe protein can be formed [25] allows investigation of the key parameters in this complex biohybrid, including the impact of different hole-scavenger electron donors.

In the initial studies of CdS-MoFe protein biohybrids, the SED was the buffer HEPES or ascorbic acid (AA) [19,20,26,27]. These two SEDs have limitations, including HEPES being expensive and formation of oxidized AA radicals that disproportionate to limit recycling with the possible formation of damaging side reactions [28]. Additionally, both SEDs are used in high concentrations, resulting in high ionic strengths in solution, which can alter the colloidal stability of the electrostatically-stabilized nanocrystal-enzyme complexes. Herein, the role of different SED molecules on the overall rate of light-driven N_2 reduction in a CdS QD-MoFe protein biohybrid was examined. It is shown that different SED can have an impact on the overall rate of N_2 reduction catalyzed by this system, demonstrating that optimization of the hole-scavenging reaction can improve the matching of oxidation and reduction reaction kinetics to improve the overall conversion efficiencies.

2. Results and discussion

The selection of possible SED molecules that could support N_2 reduction by a CdS QD-MoFe protein complex was first guided by small molecules with sufficiently negative standard reduction potentials to provide a thermodynamically favorable electron transfer to the valence band of CdS QD (~ + 2 V vs NHE) [26,29]. Second, the SED should not absorb light at the wavelength maximum used to excite the CdS QD (405 nm excitation) due to competition for the same incident photons that would limit efficient excitation of CdS QD and subsequent productive electron transfer to MoFe protein. Third, the oxidized SED should be readily reduced by a sustainable chemistry, such as electrochemically. Finally, the SED should be soluble in aqueous solutions employed for QD-MoFe protein reactions. These constraints eliminated many of the most commonly used small molecule, electron mediators employed with redox active proteins, such as the one-electron reduced viologen derivatives [30], which absorb in the visible wavelength region used to excite the CdS QD and also can be further reduced by the excited CdS QD.

Prior studies on the reactivity of the CdS QD-MoFe protein system have utilized buffer molecules (e.g., HEPES) and ascorbic acid (AA) as SEDs [19,20]. These molecules meet most of the criteria presented above. However, neither of these are readily re-reduced by sustainable processes such as reduction at an electrode. Here, three candidates were selected for comparison to the aforementioned SED molecules to function as hole scavengers in a CdS QD-MoFe protein catalyzed N_2 reduction reaction. In these studies, CdS QDs of 3.4 nm diameter with 3-mercaptopropionate (MPA) as the ligand (Fig. S1) was utilized as these nanocrystals have been demonstrated to be effective in delivering electrons to the MoFe protein to support N_2 reduction [20,21,31,32]. Dithionite (DT) is a commonly used reductant [33]. Triethanolamine (TEOA) has been utilized as an SED for other photo-driven redox systems [22,34]. Likewise, hydroquinone (HQ) is representative of a large family of compounds that have desirable properties for use as a SED, including accessible reduction by electrodes [22,35–38].

Initially, the ability of DT, TEOA, and HQ to support N_2 reduction activity by a CdS QD-MoFe protein complex were compared to AA at a fixed time (60 min) and a single SED concentration (50 mM). As can be seen in Fig. 2, 50 mM DT, AA, and TEOA all supported significantly higher rates of N_2 reduction by the complex compared to 5 mM DT. Furthermore, 50 mM HQ supported a significantly higher N_2 reduction activity (~50% increase) compared to the other SEDs that were tested. These findings reveal that use of AA as a SED does not result in optimal rates of N_2 reduction catalyzed by this biohybrid system and point to HQ as a better choice as an SED.

Next, the dependence of the rates of N_2 reduction by the biohybrid system on the concentration of the different SED was examined (Fig. 3).

Dithionite shows an initial increase in rate followed by a decrease in rate across the concentration range, with a maximum rate observed at 50 mM and a significant decrease in the rate at higher concentrations (100 mM). This decrease in activity is expected to result from the increase in solution ionic strength, which is known to interfere with the formation of the CdS-MoFe protein complex [21]. Ascorbic acid and TEOA show a steady increase in N_2 reduction across the concentration range up to 100 mM, consistent with previous studies [26]. HQ demonstrated an increase in N_2 reduction rate up to 50 mM followed by a decrease in rate. The maximum rate supported by HQ at 50 mM, ~180 nmol NH_3/nmol MoFe protein/h, was 1.5-fold higher than that observed for DT at 50 mM, and comparable to the rates observed for TEOA and AA at 100 mM. Taken together, these results demonstrate that in earlier studies, use of AA as the SED led to limiting hole scavenging reaction kinetics and lower overall N_2 reduction rates. The overall rates of N_2 reduction can be significantly enhanced by using optimal concentrations of a non-ionic SED that minimize electrostatic effects that have been shown to inhibit binding to the negatively charged surface of the MPA-capped QD [25]. Further, it is clear that the new SEDs examined here, DT, TEOA, and HQ, can function as effective hole scavengers, with HQ being particularly interesting since it supports the highest rates of N_2 reduction by the complex at the modest concentration of 50 mM. Further, a large family of HQ derivatives are readily available and are reducible via electrochemical methods [35–38].

The reduction of N_2 to NH_3 in these studies was quantified by analysis of NH_3 using a fluorescence assay with reference to a NH_4Cl standard curve [39], which was further confirmed using an $^{15}NH_3/^{1}H$ NMR assay [20]. In this assay, $^{15}N_2$ is used as the substrate and the product $^{15}NH_3$ was quantified using ^{1}H NMR, as previously described [40]. As shown in Figs. S2-S5, the quantification of NH_3 by both the fluorescence and NMR detection methods were very similar, confirming that the fluorescence detection method used in these studies is accurately measuring N_2 reduction.

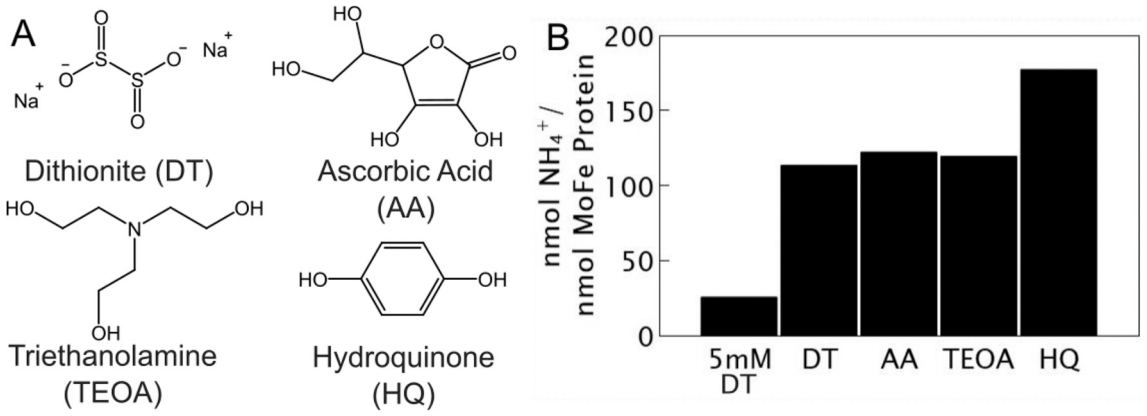

Fig. 2. Electron donor structures shown (panel A). Ammonia production by CdS QD-MoFe protein in the presence of various electron donors (panel B). Samples were prepared by mixing 50 mM MOPS pH 7.0, 5 mM sodium dithionite, 0.5 μM CdS QD-MoFe protein and the specified electron donor at 50 mM. Assays were run by illuminating for 1 h at a wavelength of 405 nm and an output power of 30 mW.

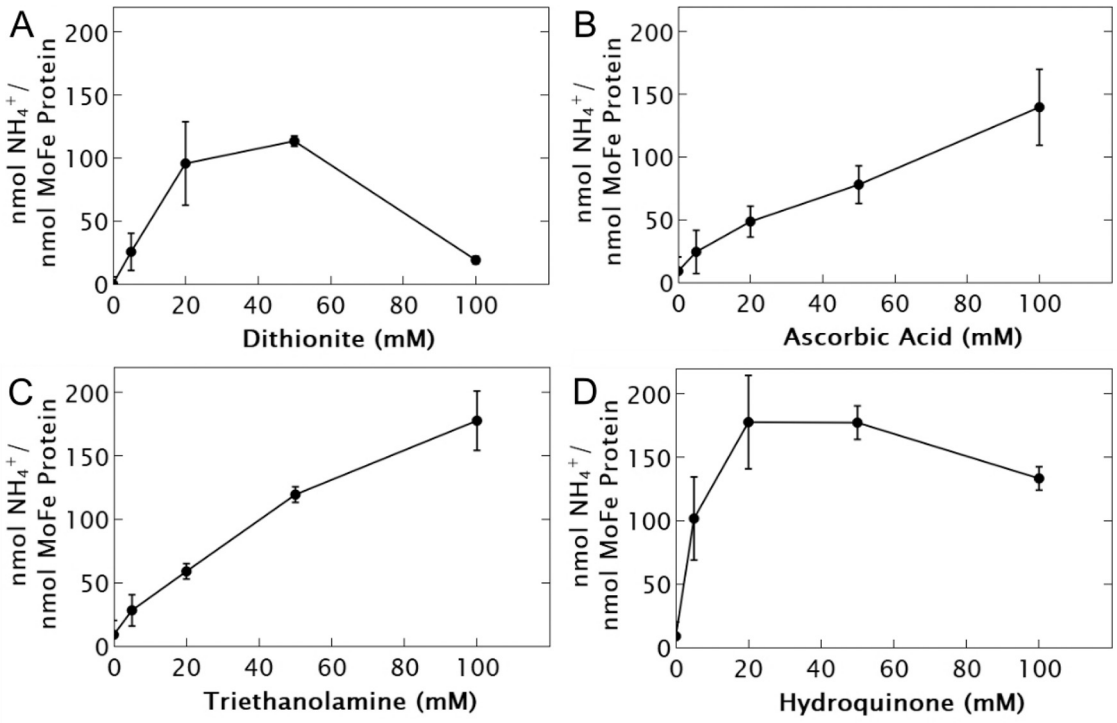

Fig. 3. Product formation by CdS QD-MoFe protein as a function of SED concentration. Assays were performed in 50 mM MOPS pH 7.0 with 5 mM sodium dithionite (with the exception of dithionite as the only electron donor, where dithionite concentration is represented on the x-axis) and illuminated for 1 h at a wavelength of 405 nm and an output power of 30 mW. Electron donors tested were dithionite (panel A), ascorbic acid (panel B), triethanolamine (panel C), and hydroquinone (panel D).

It was of interest to establish the progress of N_2 reduction catalyzed by the CdS QD-MoFe protein complex across the time of reaction. This was established for 50 mM HQ. As shown in Fig. 4, there was an increase in NH_3 formation over time, although the rate of NH_3 formation decreases with time of reaction. The decrease in the rate of N_2 reduction is obvious when the specific activity (nmol NH_3/min/nmol MoFe protein) is plotted against the time of the reaction (Fig. 4, panel B). The non-linearity of these data suggests some important observations. First, the specific activity observed for the CdS QD-MoFe protein system at a 60 min time point greatly underestimates the initial specific activity of these systems. The initial specificity activity observed with HQ as SED at the earliest time is 6.5 nmol NH_3/min/nmol MoFe protein. That is about 4% of the maximum specific activity for N_2 reduction catalyzed by the Fe protein(2MgATP) – MoFe protein system of ~150 nmol NH_3/min/nmol MoFe protein [12]. At 60 min, the specific activity is down to 2.9 nmol NH_3/min/nmol MoFe protein. The results shown in Fig. 4 illustrate that the CdS QD-MoFe protein system loses activity over time, suggesting instability in one or more of the components under light-driven turnover conditions. This observed loss of activity could be a result of damage to the MoFe protein caused by CdS or SED radicals that are generated during light activated electron transfer reactions. Loss of activity in a CdS – hydrogenase complex was ascribed to inactivation of the hydrogenase [26]. Understanding the contributors to this instability should provide further insights into ways to stabilize the system to enable longer term sustained rates of N_2 reduction.

The effectiveness of the different SEDs examined in this study in functioning as hole scavengers for photoexcited QDs can be considered in the context of the standard reduction potentials of the SED [22,33].

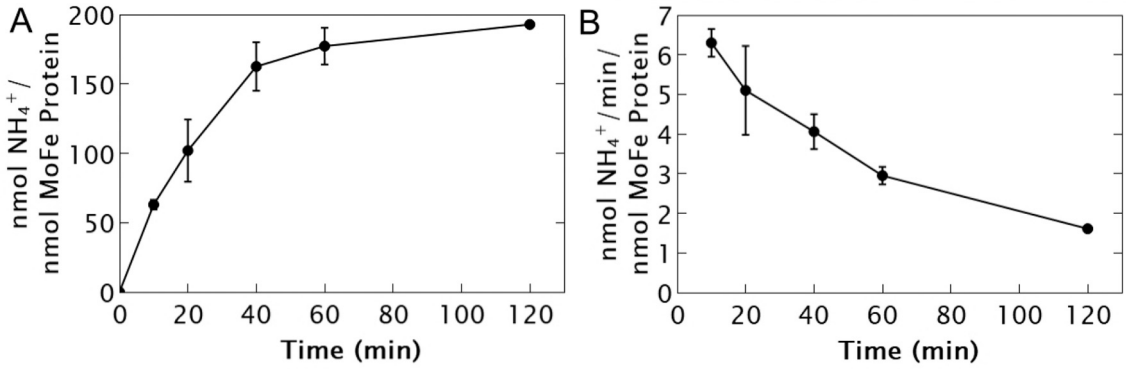

Fig. 4. Product formation (panel A) and specific activity (panel B) of CdS QD-MoFe protein as a function of time. Samples were prepared by mixing 50 mM MOPS pH 7.0, 5 mM sodium dithionite, 0.5 μM CdS QD-MoFe protein and 50 mM hydroquinone. Assays were run by illuminating for 1 h at a wavelength of 405 nm and an output power of 30 mW.

These are plotted, along with the approximate band edge potentials of the 3.4 nm CdS QD, in Fig. 5. As can be seen, all the SEDs examined here have E^0 values significantly more negative than the valence band of the CdS QD, and thus all of these SEDs have sufficient driving force for thermodynamically favorable hole-scavenging. Therefore, it is apparent that the small differences in the hole-scavenging ability of SEDs examined here to support N_2 reduction by the CdS QD-MoFe protein complex shown in Fig. 3 are not simply a result of the E^0 values. This lack of a simple potential dependence illustrates some of the complexities of the nanocrystal-enzyme systems. In addition to having different rate constants for hole scavenging, different SEDs may have different chemical interactions with the nanocrystals, which will impact the overall rate of the bimolecular hole-scavenging reaction at the same SED concentration, and the impact on the ionic strength of the solution has been shown to impact the nanocrystal-enzyme binding, which is electrostatic in nature [25]. Nonetheless, it is interesting to note that despite different chemical structures of the SEDs examined here, all support significant rates of hole scavenging, illustrating that a wide range of SEDs can work for this system. Having the ability to use a range of SEDs allows for selection of molecules that have other desirable features, such as rapid reduction at an electrode surface.

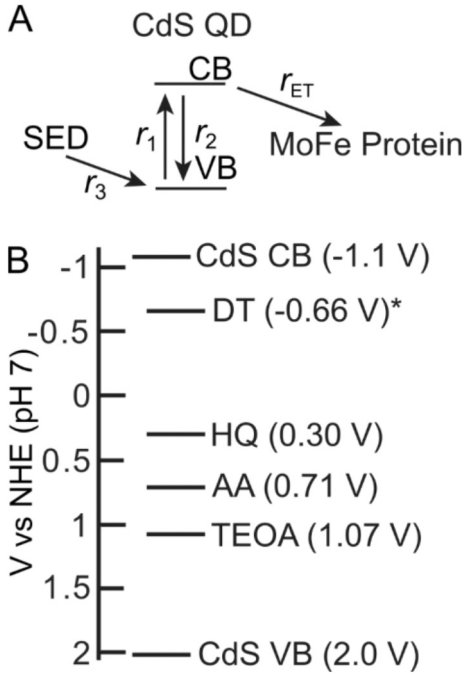

Fig. 5. Kinetic model for electron movement through the CdS QD-MoFe protein complex shown above, with reduction potentials of the conduction band and valence band of the CdS nanoparticle and the midpoint potentials of the sacrificial electron donors shown below. (The potential of dithionite is dependent on pH and concentration).

The finding here that the choice and concentration of SED can significantly alter the overall rate of N_2 reduction by the CdS QD-MoFe protein complex reveals that the rate of hole scavenging can be limiting to the overall rate of the reaction [41–44]. This observation can be considered in the context of the different rates for the important electron transfer reactions in this system (Fig. 5, panel A). The rate of electron transfer (r_{ET}) from the photo-excited CdS QD to MoFe protein plays a critical role in achieving the N_2 reduction reaction. High electron flux from CdS QD to MoFe protein complexes is critical to driving N_2 reduction, due to the flux-dependence of product formation by MoFe protein. The flux of electrons to a bound MoFe protein depends on the rate of excitation (r_1) of electrons into the CdS conduction band (CB), which is proportional to photon flux, and the probability that the electron is injected (i.e., injection efficiency). In turn, electron transfer competes with the recombination between electrons in the CB and holes in the VB (r_2), and removal of the photoexcited hole favors electron transfer to MoFe protein [21]. More effective hole scavengers should increase the lifetime of the electrons in the CB, and thus increase the quantum efficiency of electron transfer from the CdS QD to the MoFe protein, in turn increasing the rates of N_2 reduction. Additionally, hole removal prior to subsequent excitation maximizes the probability of generation of the next photoexcited electron (recall that N_2 reduction is a many-electron process). Therefore, more efficient SEDs aid N_2 reduction in at least two ways.

As already mentioned above, HQ is a representative of a large family of electrochemically recyclable quinone compounds [35–38]. The discovery here that HQ can function as effective hole-scavenging SED for a CdS-MoFe protein complex to support N_2 reduction to NH_3 illustrates how N_2 reduction can be coupled to water oxidation with light as the energy source (Fig. 6). The key missing reaction to realizing such a system was the discovery of an electron mediator (SED) that can shuttle electrons from the cathode to the VB of the CdS QD. Here it is shown that HQ is effective as an SED for the CdS-MoFe protein complex in supporting N_2 reduction. Earlier studies have demonstrated that HQ_{ox} can be readily reduced at an electrode [35–38], thus completing the circuit that would be necessary to allow the reduction of N_2 to be linked to water oxidation using light as the source of energy.

3. Conclusions

The studies presented here reveal that the SED can significantly impact the rate of hole scavenging reactions, which in turn alters the

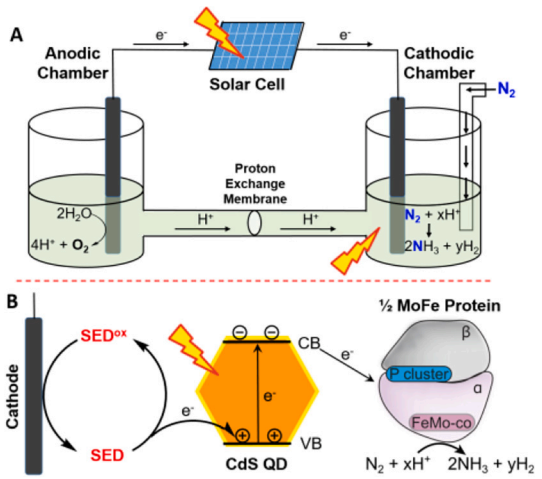

Fig. 6. Concept for coupling N_2 reduction to NH_3 coupled to water oxidation using light. Panel A shows an electrochemical cell with water oxidation occurring in the anodic chamber and N_2 reduction occurring in the cathodic chamber driven by light (solar cell). Panel B shows an expanded view of the cathode chamber reaction for integrating electron delivery from the cathode to the CdS-MoFe protein hybrid via an SED.

overall rates of N_2 reduction catalyzed by a light-driven CdS QD – MoFe protein system. Three newly employed classes of SEDs, DT, TEOA and HQ, were found to be effective hole scavengers, with some superior properties compared to the SED utilized in prior studies (AA). At a concentration of 50 mM, HQ supports a specific activity of N_2 reduction that is 50% higher than the rates observed with the other SEDs examined here. These studies clearly show that the rate of hole scavenging can be rate limiting to the overall rate of N_2 reduction in the CdS QD – MoFe protein system. It is also clear that the efficacy of the SED is not simply a function of the E^0, but rather other factors are controlling the kinetics of electron transfer from the SED to the oxidized CdS QD. The impact of hole-scavenging on the overall rate can be understood by considering the competing electron transfer pathways, with faster hole scavenging likely leading to increasing the lifetime of the photo-excited electrons in the CB of the CdS QD, thereby increasing the quantum efficiency of electron transfer and flux of electrons from the CdS QD to the MoFe protein in support of N_2 reduction. These findings provide an SED that can mediate electron transfer between an electrode and the CdS QD.

4. Experimental

4.1. General procedures

All chemicals, unless otherwise noted, were obtained from Sigma-Aldrich (St. Louis, MO) and used without further purification. Adenosine-5′-triphosphate (ATP, disodium trihydrate, Ultra-Pure) was purchased from Gold Biotechnology (St. Louis, MO). Hydrogen, argon, and nitrogen gases were purchased from Air Liquide America Specialty Gases LLC (Plumsteadville, PA). The argon and nitrogen gas were passed through an activated copper-catalyst to remove dioxygen contamination prior to use. $^{15}N_2$ gas ($\geq$ 99.8 atom% ^{15}N, $\geq$ 99%) was purchased from Sigma-Aldrich (St. Louis, MO) and used without further purification. Proteins and buffers were handled anaerobically in septum-sealed serum vials under an inert atmosphere (argon or dinitrogen), on a Schlenk vacuum line, or anaerobic glove box (Teledyne Analytical Instruments, MO-10-M, Hudson, NH). The transfer of gases and liquids were done with gastight syringes.

4.2. Nitrogenase expression and protein preparations

Molybdenum nitrogenase MoFe protein and Fe protein were expressed in *Azotobacter vinelandii* strain DJ2102 (Strep-tag MoFe protein) and DJ884, respectively. The MoFe and Fe protein were purified according to chromatographic methods described elsewhere [45]. Purified proteins were concentrated using a Millipore solvent-resistant stirred cell under an Ar atmosphere with appropriate molecular weight cutoff filters. Protein purities (>95%) was assessed using SDS-PAGE with Coomassie Brilliant Blue. Protein concentrations were determined using the Biuret method.

The proteins' activity assays were performed in 9 mL crimp-sealed vials containing 1 mL of 100 mM MOPS at pH 7.0 buffer with an ATP regeneration system (6.7 mM $MgCl_2$,30 mM phosphocreatine, 5 mM ATP, 0.2 mg/mL creatine phosphokinase, and 1.2 mg/mL BSA) with 10 mM sodium dithionite under Ar. For the specific activity of MoFe protein, 0.5 mg/mL Fe protein and 0.1 mg/mL MoFe protein were applied. For the specific activity of Fe protein, 0.125 mg/mL Fe protein and 0.5 mg/mL MoFe protein were used instead. Reactions were kept at 30 °C with constant shaking and terminated after 8 min by the addition of 300 μL of 400 mM EDTA (pH 8.0). Hydrogen gas was quantified using published methods resulting in measured specific activities of ~2000 nmol H_2 min^{-1} mg^{-1} protein for both proteins.

4.3. Nanoparticle synthesis

The 3.4 nm CdS QD was synthesized using a previously reported procedure from Hamachi et al. [46] using the sulfur precursor, O–(4-Methoxyphenyl)–O′ (p-tolyl) thiocarbonate. The cadmium oleate precursor was synthesized using a modified previously described procedure [47,48]. CdO (5 mmol) and acetonitrile (4 mL) were added to a 25 mL Erlenmeyer flask and stirred at 0 °C in an ice bath. While stirring, trifluoroacetic anhydride (5 mmol) and trifluoroacetic acid (1 mmol) were added to the CdO mixture. The solution was then removed from the ice bath and allowed to warm to room temperature overnight. This resulted in a clear and colorless solution. Then oleic acid (10.05 mmol) and triethylamine (11.3 mmol) were added to dichloromethane (20 mL) in a 50 mL round bottom flask. The cadmium solution was then added dropwise to the dichloromethane solution and the mixture was refluxed for one hour. The reaction was then cooled slowly to room temperature and the round bottom flask was placed in the freezer overnight to crystallize the product. The product was filtered on a glass frit and washed three times with cold methanol. After washing, the final product was collected and vacuum dried yielding a fine white power.

The O–(4-methoxyphenyl)–O′ (p-tolyl) thiocarbonate precursor was synthesized using the previously reported procedure from Hamachi et al. [46] Briefly, a solution of 4-methoxyphenol in benzene and a solution of O–(p-tolyl) chlorothionoformate in benzene were prepared. The 4-methoxyphenol solution was added to the O–(p-tolyl) chlorothionoformate solution. Then pyridine was added dropwise, with the solution color changing from yellow to orange. The reaction mixture was then refluxed for 10 min, and the solution turned a pale-yellow color with a white crystalline precipitate. The colored benzene solution was then washed with water, saturated brine, and then dried over sodium sulfate. The final product was collected by removing the volatiles in vacuo yielding a white powder. The product was recrystallized using methanol.

Cadmium oleate (0.244 g), 99% oleic acid (0.226 g), and hexadecane (20.10 g) were added to a 50 mL three neck round bottom flask. The mixture was then heated to 90 °C and placed under vacuum for 1 h. The solution was then placed under argon and heated to 240 °C. Once at 240 °C, the O – (4-methoxyphenyl) – O′ (p-tolyl) thiocarbonate solution (0. 0822 g in 1.50 mL diphenyl ether) was injected and the QDs grew for 45 min. The QDs were then precipitated with acetone, centrifuged, and the supernatant was removed. The QDs were then dissolved in hexanes. The unreacted cadmium oleate was removed by precipitation with the addition of acetone in 0.5 mL increments. The solution was then centrifuged for 1 min to separate the unreacted cadmium oleate from the supernatant. The supernatant was collected and the QDs were

precipitated with additional acetone. The solution was centrifuged, and the supernatant was discarded. The QDs were then washed with toluene/methanol two additional times. The final oleate capped CdS QDs were dissolved in 500 μL of anhydrous toluene and stored in the glovebox before being ligand exchanged.

The 3-mercaptopropionic acid (MPA) ligand exchange follows a previously reported procedure [26]. In the glovebox, the native-oleate capped CdS QDs were added into ~1 mL of anhydrous toluene. MPA (0.136 g) and tetramethylammonium hydroxide (0.300 g) were added to 15.00 g of methanol. The MPA methanol solution (700 μL) was added to the QDs in toluene. The solution then turned optically transparent, indicating the native oleate ligands exchanged to MPA. The QDs were then transferred to a 50 mL centrifuge tube and approximately 1 mL of methanol was used to rinse out any remaining QDs in the glass vial. The QDs were then precipitated using anhydrous toluene (~35 mL) and collected using centrifugation. The QDs were then dried under vacuum and the final product was then redissolved in Millipore water and stored under an Ar atmosphere until use.

4.4. Photochemical substrates reduction assays of CdS:MoFe protein biohybrid system

All photochemical reactions were conducted in septum-sealed transparent vials with a total volume of 1.5 mL containing 500 μL of 50 mM MOPS buffer at pH 7.0 with different electron donors, the concentrations of which are specified in Figure legends. Regardless of the SED added, all reaction mixtures contained 5 mM dithionite. Illumination of all reaction mixtures was performed with a 405 nm LED diode light source (Ocean Optics) at ~30 mW (~ 4.9 mW cm^{-2} at the sample). For a typical procedure, samples were prepared in glovebox under argon. Assay buffer was prepared by mixing a stock solution of 50 mM MOPS at pH 7.0 with 100 mM SED in 50 mM MOPS at pH 7.0. A 1:1 ratio of CdS:MoFe protein was prepared by addition of 500 nM CdS and 500 nM MoFe protein to the assay buffer containing the specified SED. N_2 turnover samples were degassed on a Schlenk line and put under natural abundant N_2 or $^{15}N_2$. Prepared samples were illuminated for 60 min with constant stirring. Ammonia was quantified using the fluorescence method as described previously [39] or a ^{1}H NMR method [20,40]. Samples for ^{1}H NMR quantification of ammonia were prepared by addition of 1 M H_2SO_4 to the reaction solution to achieve a final concentration of 0.1 M H_2SO_4. Samples were then vortexed and centrifuged at 14,000 RPM for 5 min and the supernatant was collected for ^{1}H NMR analysis done using a Bruker Avance III 500 MHz spectrometer equipped with a Bruker TXI triple resonance probe. Spectra were acquired at 298 K with 512 scans with 10% deuterium oxide (D_2O) added into an inserted capillary tube as the locking agent. The concentrations of the ammonia were determined by comparison of the peak areas to a standard curve generated with either $^{14}NH_4^+$ or $^{15}NH_4^+$.

CRediT authorship contribution statement

Andrew Clinger: Conceptualization, Data curation, Formal analysis, Investigation, Methodology. **Zhi-Yong Yang:** Conceptualization, Writing – original draft, Writing – review & editing. **Lauren M. Pellows:** Investigation, Writing – review & editing. **Paul King:** Conceptualization, Writing – review & editing, Funding acquisition. **Florence Mus:** Conceptualization, Data curation, Writing – review & editing. **John W. Peters:** Conceptualization, Writing – review & editing, Funding acquisition. **Gordana Dukovic:** Conceptualization, Writing – review & editing, Funding acquisition. **Lance C. Seefeldt:** Conceptualization, Formal analysis, Funding acquisition, Project administration, Supervision, Writing – original draft, Writing – review & editing.

Declaration of competing interest

The authors declare that they have no known competing financial interests or personal relationships that could have appeared to influence the work reported in this paper.

Data availability

Data will be made available on request.

Acknowledgements

Funding was provided by the U.S. Department of Energy Office of Basic Energy Sciences, Division of Chemical Sciences, Geosciences, and Biosciences, Physical Biosciences and Solar Photochemistry Programs. This work was authored in part by the Alliance for Sustainable Energy, LLC, the manager, and operator of the National Renewable Energy Laboratory for the U.S. Department of Energy (DOE) under Contract No. DEAC36-08GO28308. The U.S. Government and the publisher, by accepting the article for publication, acknowledges that the U.S. Government retains a nonexclusive, paid-up, irrevocable, worldwide license to publish or reproduce the published form of this work, or allow others to do so, for U.S. Government purposes.

References

[1] X. Zhang, B.B. Ward, D.M. Sigman, Chem. Rev. 120 (2020) 5308–5351.
[2] H.R. Rucker, B. Kaçar, Trends Microbiol. (2023) (in press.).
[3] S.D. Threatt, D.C. Rees, FEBS Lett. 597 (2023) 45–58.
[4] L.C. Seefeldt, Z.-Y. Yang, D.A. Lukoyanov, D.F. Harris, D.R. Dean, S. Raugei, B. M. Hoffman, Chem. Rev. 120 (2020) 5082–5106.
[5] A.J. Jasniewski, C.C. Lee, M.W. Ribbe, Y. Hu, Chem. Rev. 120 (2020) 5107–5157.
[6] B.K. Burgess, D.J. Lowe, Chem. Rev. 96 (1996) 2983–3012.
[7] B.M. Hoffman, D. Lukoyanov, Z.-Y. Yang, D.R. Dean, L.C. Seefeldt, Chem. Rev. 114 (2014) 4041–4062.
[8] O. Einsle, D.C. Rees, Chem. Rev. 120 (2020) 4969–5004.
[9] H.L. Rutledge, F.A. Tezcan, Chem. Rev. 120 (2020) 5158–5193.
[10] C. Van Stappen, L. Decamps, G.E. Cutsail, R. Bjornsson, J.T. Henthorn, J.A. Birrell, S. DeBeer, Chem. Rev. 120 (2020) 5005–5081.
[11] L.C. Seefeldt, B.M. Hoffman, J.W. Peters, S. Raugei, D.N. Beratan, E. Antony, D. R. Dean, Acc. Chem. Res. 51 (2018) 2179–2186.
[12] Z.-Y. Yang, R. Ledbetter, S. Shaw, N. Pence, M. Tokmina-Lukaszewska, B. Eilers, Q. Guo, N. Pokhrel, V.L. Cash, D.R. Dean, E. Antony, B. Bothner, J.W. Peters, L. C. Seefeldt, Biochemistry 55 (2016) 3625–3635.
[13] Z.-Y. Yang, A. Badalyan, B.M. Hoffman, D.R. Dean, L.C. Seefeldt, J. Am. Chem. Soc. 145 (2023) 5637–5644.
[14] J.G. Chen, R.M. Crooks, L.C. Seefeldt, K.L. Bren, R.M. Bullock, M.Y. Darensbourg, P.L. Holland, B. Hoffman, M.J. Janik, A.K. Jones, M.G. Kanatzidis, P. King, K. M. Lancaster, S.V. Lymar, P. Pfromm, W.F. Schneider, R.R. Schrock, Science 360 (2018) eaar6611.
[15] W. Gu, R.D. Milton, Chemistry 2 (2020) 322–346.
[16] K. Danyal, A.J. Rasmussen, S.M. Keable, B.S. Inglet, S. Shaw, O.A. Zadvornyy, S. Duval, D.R. Dean, S. Raugei, J.W. Peters, L.C. Seefeldt, Biochemistry 54 (2015) 2456–2462.
[17] K. Danyal, B.S. Inglet, K.A. Vincent, B.M. Barney, B.M. Hoffman, F.A. Armstrong, D.R. Dean, L.C. Seefeldt, J. Am. Chem. Soc. 132 (2010) 13197–13199.
[18] D.P. Hickey, R. Cai, Z.-Y. Yang, K. Grunau, O. Einsle, L.C. Seefeldt, S.D. Minteer, J. Am. Chem. Soc. 141 (2019) 17150–17157.
[19] K.A. Brown, D.F. Harris, M.B. Wilker, A. Rasmussen, N. Khadka, H. Hamby, S. Keable, G. Dukovic, J.W. Peters, L.C. Seefeldt, P.W. King, Science 352 (2016) 448–450.
[20] K.A. Brown, J. Ruzicka, H. Kallas, B. Chica, D.W. Mulder, J.W. Peters, L.C. Seefeldt, G. Dukovic, P.W. King, ACS Catal. 10 (2020) 11147–11152.
[21] J.L. Ruzicka, L.M. Pellows, H. Kallas, K.E. Shulenberger, O.A. Zadvornyy, B. Chica, K.A. Brown, J.W. Peters, P.W. King, L.C. Seefeldt, G. Dukovic, J. Phys. Chem. C 126 (2022) 8425–8435.
[22] Y. Pellegrin, F. Odobel, C. R. Chim. 20 (2017) 283–295.
[23] A.W. Mureithi, Y. Sun, T. Mani, A.R. Howell, J. Zhao, Cell Rep. Phys. Sci. 3 (2022) 100889.
[24] D. Guerrero-Araque, P. Acevedo-Peña, D. Ramírez-Ortega, R. Gómez, New J. Chem. 41 (2017) 12655–12663.
[25] L.M. Pellows, M.A. Willis, J.L. Ruzicka, B.P. Jagilinki, D.W. Mulder, Z.-Y. Yang, L. C. Seefeldt, P.W. King, G. Dukovic, J.W. Peters, Nano Lett. 22 (2023) 10466–10472.
[26] K.A. Brown, M.B. Wilker, M. Boehm, G. Dukovic, P.W. King, J. Am. Chem. Soc. 134 (2012) 5627–5636.
[27] J.K. Utterback, M.B. Wilker, K.A. Brown, P.W. King, J.D. Eaves, G. Dukovic, Phys. Chem. Chem. Phys. 17 (2015) 5538–5542.
[28] Y.-J. Tu, D. Njus, H.B. Schlegel, Org. Biomol. Chem. 15 (2017) 4417–4431.
[29] H.-W. Tseng, M.B. Wilker, N.H. Damrauer, G. Dukovic, J. Am. Chem. Soc. 135 (2013) 3383–3386.

[30] A. Badalyan, Z.-Y. Yang, B. Hu, J. Luo, M. Hu, T.L. Liu, L.C. Seefeldt, Biochemistry 58 (2019) 4590–4595.
[31] B. Chica, J. Ruzicka, L.M. Pellows, H. Kallas, E. Kisgeropoulos, G.E. Vansuch, D. W. Mulder, K.A. Brown, D. Svedruzic, J.W. Peters, G. Dukovic, L.C. Seefeldt, P. W. King, J. Am. Chem. Soc. 144 (2022) 5708–5712.
[32] B. Chica, J. Ruzicka, H. Kallas, D.W. Mulder, K.A. Brown, J.W. Peters, L.C. Seefeldt, G. Dukovic, P.W. King, J. Am. Chem. Soc. 142 (2020) 14324–14330.
[33] S.G. Mayhew, Eur. J. Biochem. 85 (1978) 535–547.
[34] C. Kutal, M.A. Weber, G. Ferraudi, D. Geiger, Organometallics 4 (1985) 2161–2166.
[35] A. Rodenberg, M. Orazietti, M. Mosberger, C. Bachmann, B. Probst, R. Alberto, P. Hamm, ChemPhysChem 17 (2016) 1321–1328.
[36] M.T. Huynh, C.W. Anson, A.C. Cavell, S.S. Stahl, S. Hammes-Schiffer, J. Am. Chem. Soc. 138 (2016) 15903–15910.
[37] L. Mtemeri, D.P. Hickey, J. Phys. Chem. B 127 (2023) 7685–7693.
[38] R.D. Milton, D.P. Hickey, S. Abdellaoui, K. Lim, F. Wu, B. Tan, S.D. Minteer, Chem. Sci. 6 (2015) 4867–4875.
[39] B.M. Barney, J. McClead, D. Lukoyanov, M. Laryukhin, T.-C. Yang, D.R. Dean, B. M. Hoffman, L.C. Seefeldt, Biochemistry 46 (2007) 6784–6794.
[40] N.E. Preece, S. Cerdan, Anal. Biochem. 215 (1993) 180–183.
[41] K. Wu, Z. Chen, H. Lv, H. Zhu, C.L. Hill, T. Lian, J. Am. Chem. Soc. 136 (2014) 7708–7716.
[42] P. Singhal, H.N. Ghosh, J. Phys. Chem. C 122 (2018) 17586–17600.
[43] N. Denisov, J. Yoo, P. Schmuki, Electrochim. Acta 319 (2019) 61–71.
[44] M.J. Berr, P. Wagner, S. Fischbach, A. Vaneski, J. Schneider, A.S. Susha, A. L. Rogach, F. Jäckel, J. Feldmann, Appl. Phys. Lett. 100 (2012) 223903.
[45] E. Jiménez-Vicente, J.S. Martin Del Campo, Z.-Y. Yang, V.L. Cash, D.R. Dean, L. C., Seefeldt, in: F. Armstrong (Ed.), Methods in Enzymology vol. 613, Academic Press, 2018, pp. 231–255.
[46] L.S. Hamachi, I. Jen-La Plante, A.C. Coryell, J. De Roo, J.S. Owen, Chem. Mater. 29 (2017) 8711–8719.
[47] M.P. Hendricks, M.P. Campos, G.T. Cleveland, I. Jen-La Plante, J.S. Owen, Science 348 (2015) 1226–1230.
[48] E. Dhaene, J. Billet, E. Bennett, I. Van Driessche, J. De Roo, Nano Lett. 19 (2019) 7411–7417.